Journal of Catalysis 278 (2011) 200–207

Contents lists available at ScienceDirect

Journal of Catalysis

journal homepage: www.elsevier.com/locate/jcat

Complex intermetallic compounds as selective hydrogenation catalysts – A case study for the (100) surface of $Al_{13}Co_4$

Marian Krajčí [a,b], Jürgen Hafner [a,*]

[a] Fakultät für Physik and Center for Computational Materials Science, Universität Wien, Sensengasse 8, Wien 1090, Austria
[b] Institute of Physics, Slovak Academy of Sciences, Dúbravská cesta, SK-84511 Bratislava, Slovak Republic

ARTICLE INFO

Article history:
Received 29 June 2010
Revised 6 December 2010
Accepted 6 December 2010
Available online 8 January 2011

Keywords:
Catalysis
Intermetallic compounds
Density-functional theory
Transition state theory
Hydrogenation
Selectivity

ABSTRACT

Recently, a novel concept for the design of selective and stable catalysts for the hydrogenation of alkynes has been announced – the isolation of the active sites on the surface of a complex intermetallic compound. The basic idea is that isolated active sites enable only a reduced number of possible adsorption geometries for the reactants, leading to a narrower range of possible reaction products. However, so far an atomistic scenario for the complex multi-step hydrogenation process catalyzed by complex intermetallic compounds has not yet been developed. Here, we present detailed ab initio density-functional simulations of the surface structure and of the selective hydrogenation of acetylene to ethylene on the (100) surface of the compound $Al_{13}Co_4$. In agreement with recent STM investigations, our calculations show that the surface is highly corrugated with well-separated Co surface atoms in the center of $CoAl_5$ pentagons. The activation energies for the rate-controlling steps are found to be comparable or even lower than those calculated for conventional Pd or Pd–Ag catalysts, and the desorption energy of ethylene is lower than the barrier to further hydrogenation to ethyl. This confirms that $Al_{13}Co_4$ is an efficient as well as highly selective catalyst. Our results demonstrate that the active sites are not the Co atoms alone, but pentagonal $CoAl_5$ clusters forming zig-zag chains on the surface separated by wide troughs. The high activity of the Al atoms in these clusters is promoted by the strong, partially covalent bonding between Al and Co atoms, as well as by their low coordination in a surface with a very complex topology.

1. Introduction

Ethylene produced by a steam cracking process typically contains up to 1% of acetylene. In the ethylene feedstock used for the production of polymers, the acetylene content has to be reduced to a few ppm to avoid poisoning of the polymerization catalyst [1]. The removal of acetylene is usually achieved by Pd-based hydrogenation catalysts. To avoid a further hydrogenation of ethylene to ethane requires a strong modification of the near-surface region of Pd. Pd catalysts modified by the addition of Ag have been found to be highly selective and are widely used industrially [2], and other Pd-based catalysts (Pd–Au [3], Pd–Pb [4], Pd–Ga [5–8]) have also been found to be highly selective. Recently, it has been demonstrated that pure Pd catalysts can be selective if the reaction is performed under conditions where subsurface carbon is formed [9,10]. However, all Pd-based catalysts share the disadvantage of high cost. Using extensive screening based on density-functional calculations, Studt et al. [11] have identified Ni–Zn alloys as an efficient selective hydrogenation catalyst free of precious metals, and the predicted high selectivity was also confirmed experimentally. In a very recent conference presentation, Armbrüster et al. [12–14] reported that also the complex intermetallic compound $Al_{13}Co_4$ is an efficient and highly selective hydrogenation catalyst for alkynes.

In contrast to the conventional selective hydrogenation, catalysts based on Pd or disordered substitutional Pd-based alloys were the active transition-metal sites are densely and randomly distributed over the exposed surface, the transition-metal sites in the ordered intermetallic compounds PdGa (crystallizing in the B20 structure [15]), $Al_{13}Co_4$ (crystal structures oP102 [16] or mC102 [17]) and possibly also $Ni_{16}Zn_{53}$ (crystal structure oB138 [18] – although this compound has not yet been uniquely identified as the catalytically active phase) are coordinated only by simple metal atoms. This has motivated Kovnir et al. [5] to announce the isolation of the active sites as a new concept for the rational design of novel catalysts. The high selectivity of these compounds as hydrogenation catalysts has been attributed to the preferential formation of weakly π-bonded adsorbed acetylene bound to the transition-metal atoms and a reduced amount of di-σ-bonded acetylene and adsorbed ethylene and ethylidyne species [5,6]. In addition, the importance of the control of the surface structure with a view of controlling the local structure around the active site has been emphasized [7,8,19].

* Corresponding author. Fax: +43 1 4277 9514.
E-mail address: juergen.hafner@univie.ac.at (J. Hafner).

0021-9517/$ - see front matter © 2010 Elsevier Inc. All rights reserved.
doi:10.1016/j.jcat.2010.12.004

In general, the reaction path for the hydrogenation of acetylene is thought to follow a Horuiti–Polanyi scheme where a series of hydrogenated C_2H_x species are formed by the sequential addition of dissociatively adsorbed hydrogen atoms to the co-adsorbed hydrocarbon intermediate. This means that besides the active sites binding the hydrocarbon, other active sites must be present which promote the dissociative adsorption of hydrogen. For Pd and Pd–Ag catalysts, Neurock et al. [20] have performed a detailed ab initio density-functional investigation of the hydrogenation process, followed by kinetic Monte Carlo studies [21]. Their analysis has demonstrated that electronic effects (changes in the local densities of states upon alloying) are far less important for promoting an enhanced selectivity than geometric effects. Increased coordination of Pd by Ag reduces the adsorption energies, but the desorption energy of ethylene is still higher than the barrier to a further hydrogenation of ethane. The observed selectivity has been attributed to an activation energy for the de-hydrogenation of ethyl to ethylene that is much lower than the barrier for further hydrogenation of ethyl to ethane. However, with increasing Ag content, dissociative adsorption of hydrogen becomes less favorable such that an optimal Pd/Ag ratio and coordination is required to achieve both high activity and selectivity.

Here, we present a detailed investigation of the selective hydrogenation of acetylene to ethylene on the (100) surface of the complex intermetallic compound $Al_{13}Co_4$ using ab initio density-functional theory. To model a multi-step catalytic reaction on the surface of an intermetallic compound is a much more challenging task than describing a similar reaction on a close-packed surface of a metal. In contrast to the well-studied low-index surfaces of metals or random alloys, our knowledge of the surfaces of complex intermetallic compounds is still rather limited. Under these circumstances, it is a happy coincidence that the (100) surface of $Al_{13}Co_4$ has recently been studied in detail by scanning tunneling microscopy (STM) and density-functional calculations [22]. We have extended these investigations by constructing a realistic model of the surface structure generated by a simulated cleavage experiment, leading to very good agreement with the STM investigations. The surface of the compound is found to be highly corrugated, with chains of Co-centered $CoAl_5$ pentagons protruding from a flatter Co-richer layer. The optimal configurations for (co)adsorbed hydrogen and hydrocarbon molecules on both parts of the surface have been determined, and a complete energetic profile for all steps of the sequential hydrogenation of acetylene to vinyl, ethylene, ethyl, and ethane has been derived. While the adsorption energies for hydrocarbon molecules on the protruding $CoAl_5$ pentagons and on the exposed regions of the flat underlayer are comparable, the activation energy for the hydrogenation of acetylene to vinyl is only 63 kJ/mol for molecules adsorbed on the pentagons, but 151 kJ/mol for molecules adsorbed on the lower layer. Hydrogenation will hence take place almost exclusively on the protruding parts of the surface. The high selectivity of $Al_{13}Co_4$ is shown to arise from a change in the adsorbate–substrate bonding: While acetylene and vinyl are bound to two Al atoms close to an isolated Co atom in a di-σ configuration, ethylene, ethyl, and ethane are π-bonded on top of a Co atom. The change in the adsorption mode leads to a desorption energy for ethylene which is lower than the activation energy for the next hydrogenation step and explains the observed selectivity of the catalyst.

2. Computational methods

Density-functional calculations were carried out using the VASP code [23] that uses a plane-wave basis (cut-off energy 700 eV), the projector-augmented-wave (PAW) method to describe core electrons [24], and performs an iterative diagonalization of the Kohn–Sham Hamiltonian. The calculations were performed in the generalized gradient approximation, using the Perdew–Wang functional [25]. The self-consistency iterations were stopped when total energies are converged to within 10^{-6} eV. The optimized geometries of the surface and of the adsorbate–substrate complexes were determined using static relaxations using a quasi-Newton method and the Hellmann–Feynman forces acting on the atoms. Transition states were determined using the nudged-elastic band method [26]. In structural optimizations and transition-state searches, convergence criteria of 10^{-4} eV for total energies and 0.1 eV/Å for forces acting on the atoms were applied.

The stable (100) surface of orthorhombic $Al_{13}Co_4$ was determined using a simulated cleavage experiment. The surface was modeled by a symmetric slab consisting of seven atomic layers, separated by a 16 Å wide vacuum layer. The computational cell contained 153 atoms in the slab plus the atoms of the adsorbed species. Only the Γ point was used for exploratory calculations of different adsorption configurations, but for the determinations of the potential-energy profile of the reaction, Brillouin-zone integrations were based on a $2 \times 2 \times 1$ k-point mesh. Changes of the adsorption energies relative to the Γ-point-only values were modest, and the satisfactory convergence of the total energies was further checked by calculations for the clean substrate using a finer $4 \times 4 \times 1$ mesh.

3. (100) surface of orthorhombic $Al_{13}Co_4$

The crystal structure of $Al_{13}Co_4$ has been determined by Grin et al. [16] using X-ray diffraction by single-crystal and powder specimens. The structure is orthorhombic (Pearson symbol oP102, space group $Pmn2_1$, No. 31). The lattice parameters are $a = 8.158$ Å, $b = 12.342$ Å, and $c = 14.452$ Å, and the unit cell contains 102 atoms (78 Al and 24 Co). According to Henley [27], the elementary building block of the structure is a large 23-atom cluster forming a pentagonal bipyramid (PB). Each PB consists of a flat equatorial layer consisting of a decagonal ring of alternating Al and Co atoms centered by a single Al atom and two puckered capping layers consisting of an Al pentagon centered by a Co atom. Neighboring PB's are joined by flat junction layers. Together, the structure can also be described in terms of an alternating stacking of flat (F) and puckered (P) layers. The structure of $Al_{13}Co_4$ has received considerable attention because it represents an approximant phase to decagonal Al–Co and Al–Ni–Co quasicrystals [30]. Using ab initio total-energy and molecular dynamics simulations, Mihalkovič and Widom [31] have explored the importance of entropic contributions in the stabilization of the structure; the electronic structure has been discussed by Krajčí and Hafner [32]. The $Al_{13}Co_4$ compound has also interesting anisotropic electronic transport properties [33].

Orthorhombic $Al_{13}Co_4$ cleaves preferentially along (100) planes. Because of the layered structure, one would expect the cleavage to occur between the F and P layers. The (100) surface has been investigated by Addou et al. [22] using low-energy electron diffraction and scanning tunneling microscopy (STM). The STM experiments show that the surface termination corresponds either to an incomplete puckered (P) layer or to an incomplete flat (F) layer whose alternating stacking defines the crystal structure of the compound. The local atomic arrangements present in the bulk were found to be preserved at the free surface, no reconstruction or surface segregation has been detected [22].

We have performed a simulated cleavage experiment using the Hellmann–Feynman forces from the ab initio density-functional calculations. The computer experiment was performed by applying an increasing uniaxial tensile strain in the (100) direction perpendicular to the layers and relaxing forces and lateral stresses. The result demonstrates that cleavage occurs by splitting the P layer

into two parts attached to the upper and lower surfaces (see Fig. 1) such that the integrity of the PB's is preserved.

The fully relaxed stable surface (see Fig. 2) exposes pentagonal rings of Al atoms centered by Co atoms. These pentagonal rings are part of large pentagonal bipyramids (PB's) that have been described by Henley [27] as the building blocks of the $Al_{13}Co_4$ crystal structure. The flat equatorial plane of the PB's is occupied by a central Al atom surrounded by a decagonal ring of Co and Al atoms, capped on both sides by $CoAl_5$ pentagons with a slightly protruding central Co atom.

The PB's are stabilized by strong, partially covalent Co–Al bonds. Recent nuclear magnetic resonance (NMR) studies [28,29] have identified two ^{27}Al signals, one has been attributed to Al atoms in the outer shell of the PB's, the second with an exceptionally large axially symmetric quadrupole splitting to Al atoms in the center of the PB's. The large splitting arises from the strong bonding between the Al atom in the center of the PB and the Co atoms in the capping pentagons.

The surface structure can be described in terms of a tiling with pentagons and thin rhombi or alternatively with squashed hexagons. Only half of the pentagons and rhombi are decorated with Co-centered Al pentagons or Al atoms, they are separated by wide troughs. The strongly corrugated structure of the surface is a surprising result – as shall be demonstrated below, the surface topology is of foremost importance for understanding its catalytic properties. Co atoms (which are expected to form the catalytically active sites) appear in the center of pairs of $CoAl_5$ pentagons; they are separated by a distance of 6.15 Å (the length of the edge of a hexagonal tile). The strong Co–Al binding inside the pentagonal bipyramids is reflected by short Co–Al distances of 2.21 Å within the Co-centered $CoAl_5$ pentagons.

In contrast to the incomplete P layer forming the topmost surface layer that contains only isolated Co atoms, the F layer exposed in the troughs is Co-rich. Co atoms are located at all vertices of the pentagonal tiles and below the center of the pentagons. Each pentagon is decorated with a triangle of Al atoms located above the central Co atom. Two further Al atoms are located at the edges of

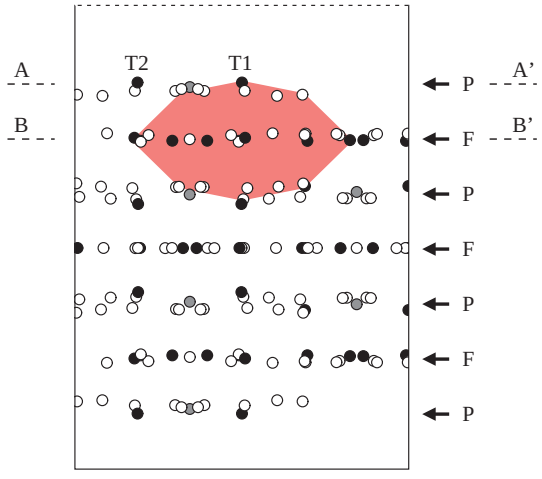

Fig. 1. Side view of the slab model for the (100) surface of $Al_{13}Co_4$ resulting from the simulated cleavage experiment. The surface layer S consists of one-half of the puckered layer (P). Part of the flat (F) layer is exposed in the regions where the P layer has been removed. The slab is symmetric with respect to the central flat (F) layer. Open circles represent Al atoms, black circles Co atoms. Gray circles represent Al sites with partial occupancies in the bulk structure. One of the pentagonal bipyramids (PB's) representing the basic building block of the structure is marked by pink (gray) shading. The charge distributions in the planes marked AA′ and BB′ are shown in Fig. 3. Labels T1 and T2 mark adsorption sites shown in Fig. 2. (For interpretation of the references to color in this figure legend, the reader is referred to the web version of this article.)

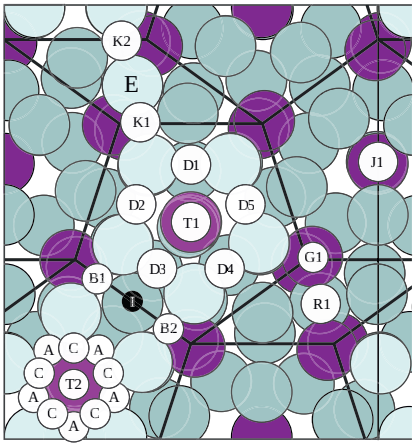

Fig. 2. Atomic structure of the (100) surface of $Al_{13}Co_4$. Al atoms in the top layer (an incomplete P layer) are shown in light blue (gray), Co atoms in magenta (dark gray). Atoms in the layers below are marked by darker shading. Possible adsorption sites on both the incomplete P layer and on the exposed part of the underlying F layer are marked by circles with capital letters. Cf. text. The Al atom marked by E easily desorbs. The surface has inversion symmetry with respect to the center I. (For interpretation of the references to color in this figure legend, the reader is referred to the web version of this article.)

the pentagon, these atoms belong to the Co–Al decagon in the equatorial plane of the PB's (see Fig. 2).

The charge-density distribution in the incomplete P layer (calculated for the plane marked AA′ in Fig. 1) shown in Fig. 3a is in good agreement with the STM picture of Addou et al. [22]. The accumulation of electron density in the Al–Al and Al–Co bonds reveals the strong, partially covalent bonding within the $CoAl_5$ pentagons. In contrast, a very low-charge density is found in the regions corresponding to the troughs. In the F layer, a rather low-charge density is found in the regions covered by the incomplete P layer. A charge-density maximum is found at the site of the Al atom in the center of the pentagon, surrounded by a ring of low electron density. In the regions of the F layer exposed at the surface, the distorted triangle of Al atoms decorating the pentagonal tile is recognized, these atoms surround a charge-density minimum in their center. In contrast to the P layer where the charge density in the thin rhombic tiles is very low, the vertices of the rhombi in the F layer are decorated with Co atoms; in addition, there are two Al atoms in each rhombus (see Fig. 3b). Surface geometry and charge-density distribution determine the adsorption properties.

4. Molecular adsorption of hydrocarbon and hydrogen molecules

To model the sequential hydrogenation process, the first steps consist in the identification of the energetically favorable adsorption sites for molecular and atomic hydrogen and for the various C_2H_x, $x = 2–6$ species. Adsorption on both the incomplete P layer and the exposed parts of the F layer has been considered. In both cases, a very large number of conceivable adsorption configurations have been examined. Because of lack of space, only the results for the most strongly binding configurations will be reported.

4.1. Adsorption on the incomplete P layer

Within the incomplete P layer exposed at the surface, there are two Co atoms per surface cell, each is surrounded by a pentagonal ring of Al atoms. As the adsorption of a hydrocarbon molecule at or close to a Co atom will block the active site for the adsorption of hydrogen, dissociative adsorption of a H_2 molecule will be possible

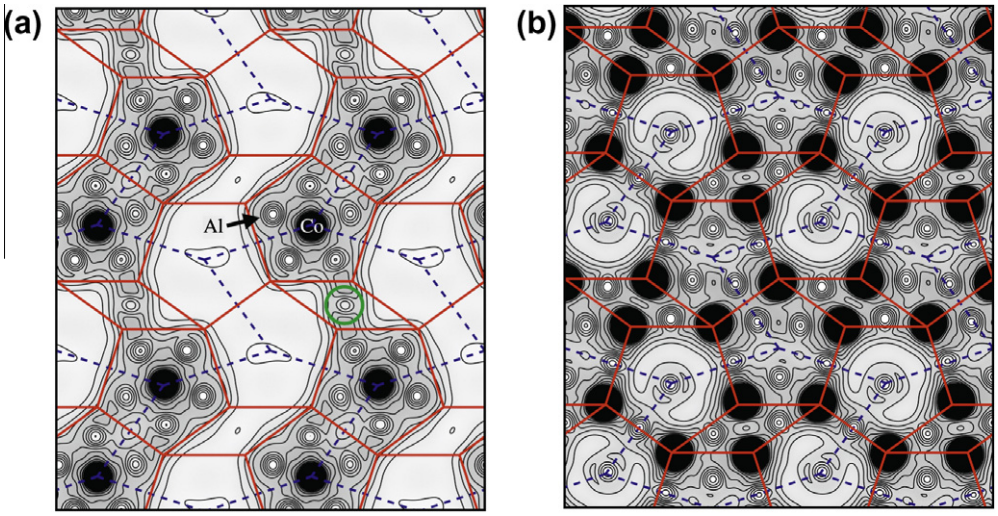

Fig. 3. Equidensity contour plot of the charge distribution in the (100) surface plane of $Al_{13}Co_4$. Panel (a) shows the charge density in the incomplete P layer. Dark regions mark the high electron density in the protruding pentagons, light gray regions the low electron density above the wide troughs. Pairs of Co-centered Al pentagons are linked through thin rhombi decorated with a single Al atom. These stripes are separated by wide troughs. Panel (b) shows the charge density in the lower F layer. In the regions covered by the incomplete P layer, the electron density is rather low (cf. text). In the exposed parts of the F layer, the charge-density distribution is determined by the Al atoms decorating the pentagonal tiles and the Co atoms located at the vertices (but remember that the Co atoms in the F layer are partially screened by the upper P layer. The surface structure may be described either in terms of a pentagon-rhombus tiling (red, full lines) or hexagon tiling (blue, dashed lines). The Al atoms in the thin rhombi of the P layer (marked by a green circle) are only weakly bound, these sites may be only partially occupied, at higher temperatures they desorb. (For interpretation of the references to color in this figure legend, the reader is referred to the web version of this article.)

only at the second Co atom. Hence, the diffusive motion of hydrogen atoms between the two sites will be an important factor controlling the activity of the catalyst.

On the topmost surface layer, molecular hydrogen is mostly strongly adsorbed on top of a Co atom (sites T1 and T2 – see Fig. 2 and Table 1). Dissociative adsorption is an activated process with a modest activation energy of 17 kJ/mol. The dissociated H atoms occupy the A and C sites around the Co atom (i.e. pseudo-threefold hollows (A) between the Co and two Al atoms or Co–Al bridge sites (C)). Possible intermediate positions along the diffusion path connecting two Co sites are the bridge sites B1 and B2 between two Al atoms, located at the edge shared by the two $CoAl_5$ pentagons. Note that the adsorption energies listed in Table 1 are given relative to molecular hydrogen in the gas phase. To obtain the actual binding energy per hydrogen atom, one-half of the molecular binding energy of −328 kJ/mol has to be added.

Acetylene is not adsorbed on top of a Co atom as might have been expected, binding is much stronger at one of the slightly inequivalent Al–Al bridge sites D1–D5 around the Co site or at the Al–Al bridge sites K1 or K2 across the shared edge of the pentagon and rhombus tiles (see Fig. 2 and Table 1). However, adsorption at sites K1 or K2 will be less important, because site E has only a fractional occupancy in the bulk and at higher temperatures Al desorbs from these sites [31]. The C_2H_3 intermediate (vinyl) is also more strongly bound at the D5 site than on top of a Co atom, only for ethylene and ethyl adsorption on top of Co is energetically favored. This is already a first important result: The adsorption of acetylene occurs not via a π-bonded configuration on top of the isolated transition-metal atom supposed to represent the "active site", but via a di-σ bond to two neighboring Al atoms whose bonding capacity is strongly enhanced (i) by a strong covalent binding with Co neighbors in the center of the pentagon and in the decagonal ring forming the central basal plane of the pentagonal bipyramid and (ii) by the low coordination of the Al atoms occupying sites at the edges of the wide troughs. Co-adsorption of a hydrocarbon species and molecular or atomic hydrogen changes the

Table 1
Adsorption energies E_{ads} (in kJ/mol, relative to the molecular species in the gas phase) of molecular and atomic hydrogen and of C_2H_x species in different sites on the $Al_{13}Co_4$ surface (see Fig. 2).

Incomplete P layer			Exposed F layer		
Adsorbate	Site	E_{ads}	Adsorbate	Site	E_{ads}
H_2	T1, T2	−46			
H	A	−22	H	G1	−28
	C	−20		R1	−18
	B1, B2	−42			
C_2H_2	T1, T2	−80	C_2H_2	J1	−186
	D1	−152		R1	−123
	D2	−161			
	D3	−181			
	D4	−182			
	D5	−184			
	K1, K2	−179			
C_2H_3	T1, T2	−202	C_2H_3	J1	−314
	D5	−322			
C_2H_4	T1, T2	−70	C_2H_4	J1	−67
C_2H_5	T1, T2	−319			

adsorption energies slightly, but does not influence the energetic order of the important adsorption configurations.

4.2. Adsorption on the exposed part of the F layer

On that part of the F layer not covered by the incomplete P layer, strong adsorption sites for acetylene are found in a threefold hollow formed by Al atoms decorating a pentagonal tile (sites J1) with an adsorption energy of −186 kJ/mol (see Table 1). This is almost exactly equal to the adsorption energy in site D5 on the incomplete P layer. In both cases, acetylene is bound in a di-σ configuration, at sites D5 in a bridging configuration between two Al atoms, at sites J1 in a configuration linking an Al atom and a bridging Al–Al site. A somewhat less favorable adsorption site is found in the center of the thin rhombi with an adsorption energy of −123 kJ/mol. Interestingly, the acetylene molecule does not form a bridge between the two Co atoms located at short distances, but is oriented perpendicular to the short diagonal of the rhombus, again in a di-σ configuration forming a bridge between two Al atoms. Adsorption of acetylene at the Co atoms occupying the vertices of the pentagonal tiles (sites G1) is not possible – here binding is sterically hindered by the Al atoms in the incomplete P layer. Vinyl and ethylene can be adsorbed only in the threefold hollows in the center of the F-pentagons, again with adsorption energies comparable to those at the energetically favored sites on the P layer. For vinyl and ethylene adsorption in the center of the thin rhombi (sites R1) or at the Co atoms occupying the vertices of the tiling (sites G1) is sterically hindered.

In contrast to the P layer, on the F layer, co-adsorption of hydrogen is possible on a pentagon with a preadsorbed acetylene molecule in its center. In this case, dissociative adsorption over a Co atom located at a vertex of a pentagon is a non-activated process. The resulting configuration consists of a di-σ-adsorbed acetylene molecule located in the central threefold hollow and two H atoms located slightly off the top position of Co atoms at the vertices with a total adsorption energy of −240 kJ/mol.

5. Energetic profile of the sequential hydrogenation of acetylene

In the next step, we simulate the sequential hydrogenation of acetylene by co-adsorbed hydrogen. As the adsorption strength of acetylene is almost the same on the incomplete P layer and on those parts of the flat F layer exposed at the surface, we have investigated hydrogenations starting from the most stable adsorption configuration on both parts of the surface. Again, we have examined a large number of conceivable reaction paths; only the results for the paths with the lowest activation energy are reported below.

5.1. Hydrogenation of acetylene to vinyl

For a reaction on the lower F layer we consider as starting configuration the most stable co-adsorption configuration with acetylene adsorbed in the center of the pentagonal tile and two hydrogen atoms bound to Co atoms located at the vertices (see Fig. 4a). For the adsorbed acetylene, the C—C bond length is stretched to 1.37 Å, the C—H bonds with the lengths of 1.10 Å are tilted away from the C–C axis by 59°, the center of the molecule is located 2.2 Å above the plane of the Al atoms in the F layer. Formation of vinyl is an exothermic process (−21 kJ/mol); but requires a rather large activation energy of 151 kJ/mol. The reaction is characterized by a late transition state, with the H atom located at 2.63 Å from the Co atom and only 1.87 Å from the C atom.

On the incomplete P layer, the starting point is acetylene adsorbed in the energetically most favorable D5 position in one pentagon, and hydrogen dissociated by adsorption on a Co atom in a neighboring pentagon. In the di-σ adsorption configuration, the acetylene molecule is strongly activated, with a C—C bond stretched to 1.40 Å and the C—H bonds tilted by 51° away from the C–C axis and from the surface. First, the co-adsorbed H atoms have to diffuse across the surface toward the adsorbed acetylene (from sites A or C via B1 to a C site close to the other Co atom). As shown by the adsorption energies compiled in Table 1, the process is essentially thermo-neutral, and the highest barrier on the diffusion path is 63 kJ/mol. In the initial state for the first hydrogenation step, the molecule is located in site D5, the two hydrogen atoms in sites C and B1 (see Fig. 5a). Along the reaction path, the H atom first moves around the Co atom, at a height of about 1.2 Å above the surface. The transition state is located above the Co atom at a height of 1.95 Å (see Fig. 5b), the activation energy for this step is 63 kJ/mol. In the final state, the H atom in the CH_2 group of vinyl is 2.4 Å above the surface.

Hence, already for the first step of the consecutive hydrogenation reactions, the activation energy for a reaction taking place on the incomplete P layer is strongly favored over a reaction on

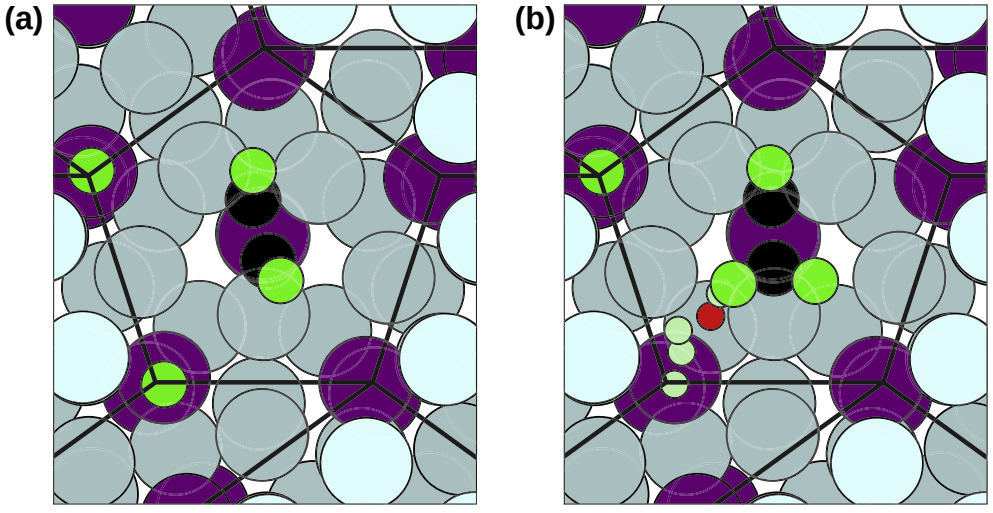

Fig. 4. (a) Co-adsorption of acetylene and hydrogen on the part of the F layer exposed at the (1 0 0) surface $Al_{13}Co_4$ (Al atoms are shown in light blue, Co atoms in deep purple, smaller circles are C atoms in black, H atoms in green). (b) Hydrogenation of acetylene to vinyl. The smallest circles indicate the displacement of the hydrogen atoms along the reaction path, the transition state is marked in red. Cf. text.

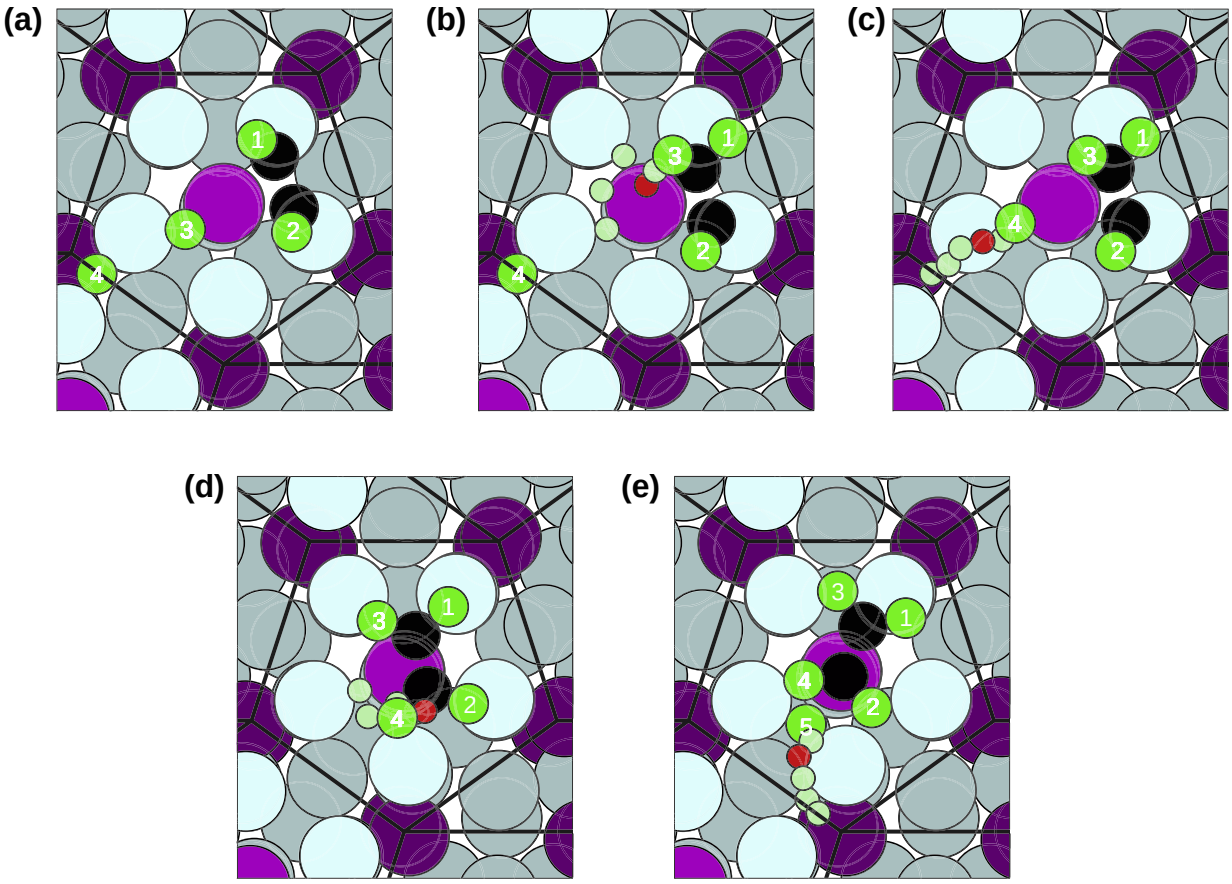

Fig. 5. Atomistic scenario for the hydrogenation of acetylene to ethylene: (a) initial state with co-adsorbed acetylene and atomic hydrogen, (b) hydrogenation of acetylene to vinyl, (c) diffusion of atomic hydrogen, (d) hydrogenation of vinyl to ethylene, and (e) rate-controlling step for the hydrogenation of ethylene to ethyl. Hydrogen atoms are numbered 1–5, black spheres represent C atoms. Small light green circles indicate the displacement of the hydrogen atoms along the reaction path, transition states are marked in red. Cf. text.

the exposed part of the F layer. Although on both parts of the surface both reactant and product have similar adsorption energies, the larger stretching of the C—C bond is a clear indication that acetylene is more strongly activated for hydrogenation on the P that on the F layer. Assuming similar prefactors, the reaction rates differ by about one order of magnitude. The further reaction will therefore be investigated only for the incomplete P layer.

5.2. Hydrogenation of vinyl to ethylene

In the next step, the fourth hydrogen atom has to move first from B1 to a C site (Co–Al bridge) where it is co-adsorbed close to the vinyl molecule, this requires to overcome a barrier of 61 kJ/mol (see Fig. 5c). Hydrogenation of vinyl to ethylene occurs by a simultaneous rotation of the C–H group of vinyl around the C–C axis and a movement of the H atom along the valley between the Co atom and the surrounding Al atoms, similar as for the first hydrogenation step. The activation energy for this step is 59 kJ/mol. In the final configuration (Fig. 5d), ethylene is bound to the Co atom in a π-bonded configuration, and the desorption energy is 70 kJ/mol. The potential-energy profile for the reaction is shown in Fig. 6.

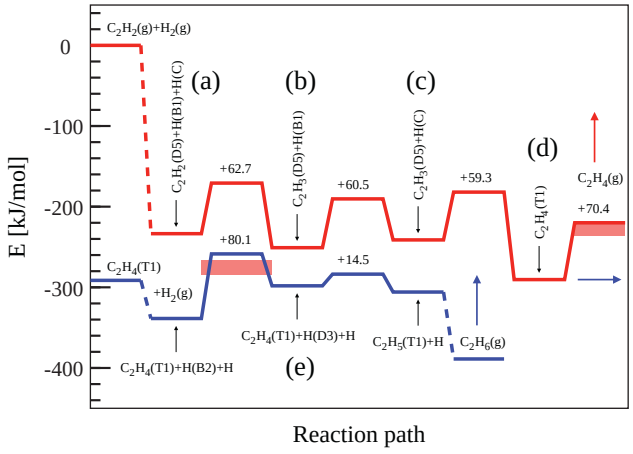

Fig. 6. Potential-energy profile for rate-controlling steps of the hydrogenation of acetylene to vinyl and ethylene (red line) and of ethylene to ethyl (blue line). The red rectangle shows the range of desorption energies for ethylene with and without co-adsorbates. The activation energy barriers are in kJ/mol. The energy scale is with respect to the reactants in the gas phase. Labels (a–e) refer to the configurations shown in Fig. 5. Cf. text. (For interpretation of the references to color in this figure legend, the reader is referred to the web version of this article.)

5.3. Hydrogenation of ethylene to ethyl

Further hydrogenation requires first the dissociative adsorption of one more hydrogen molecule, diffusion of hydrogen, reaction with ethylene to form ethyl in a first and ethane in a second hydrogenation step. The reaction path for the dissociation and diffusion is very similar to that described above. After dissociation, the two H atoms occupy position A and C around the Co atom at the T2 site, and migration of one atom from the initial site C to B2 requires an activation energy of about 60 kJ/mol. To attack the ethylene

molecule adsorbed on top of the Co atom, a hydrogen molecule has to move from B2 to a site A near the D3 site – this reaction is endothermic by 41 kJ/mol and requires an activation energy of 80 kJ/mol. Simultaneously, the ethylene molecule has to rotate slightly on top of the Co atom. In the intermediate state (see Fig. 5e), the closest distance from atom H5 to a C atom of ethylene is still 2.2 Å, and the hydrogen atom is placed only 0.8 Å above the surface. In the final reaction step resulting in the formation of adsorbed ethyl (C_2H_5), the H5 atom moves to a position 1.9 Å above the surface, 1.15 Å from the C atom. This step requires only a low activation energy of 14.5 kJ/mol and is even weakly exothermic by 7.5 kJ/mol. The essential point is that the barrier of 80 kJ/mol for the rate-controlling step (the approach of the H atom to a position close to the Co atoms were it can react with the co-adsorbed ethylene) is higher than the desorption energy of an isolated ethylene molecule of 70 kJ/mol. The desorption energy is even further lowered by co-adsorption effects. If a hydrogen atom is co-adsorbed in site B2, the desorption energy is lowered to 54 kJ/mol. The potential-energy profile for the rate-controlling steps of the hydrogenation of ethylene to ethyl, together with the desorption energy for ethylene, is represented in Fig. 6.

6. Discussion

In contrast to the stable low-index surfaces of metals or disordered alloys, cleavage of the intermetallic compound $Al_{13}Co_4$ normal to the (100) direction leads to the formation of a strongly corrugated surface consisting of an incomplete Co-poor P layer and the exposed parts of the underlying Co-rich F layer. The reason for the formation of such a strongly corrugated surface is the strong binding in the PB's , the very stable building blocks of the compound. Evidence for a strong Co–Al binding, especially along the central Co–Al–Co axis of the PB's, is also provided by the NMR experiments [28,29].

The adsorption strength of acetylene is comparable on both parts of the surface, in both cases acetylene is bound in a di-σ configuration to two (P layer), respectively, three (F layer) Al atoms decorating a pentagonal tile. Dissociative adsorption of hydrogen is a slightly activated process on the P layer, but non-activated on the F layer. On the F layer, H_2 dissociation can take place on the same pentagon, whereas on the P layer, dissociation is possible only on a neighboring pentagon. Still, for hydrogenation of acetylene to vinyl, the activation energy is more than twice as large for a reaction on the F than on the P layer. The reason is that H atoms are rather mobile on the P layer, with activation energies for diffusion of about 60 kJ/mol. Hence, a H atom can approach the adsorbed acetylene without significant loss of energy. On the F layer, a one-step reaction without preceding H-diffusion is possible. However, as binding of the H atom in locations between to Co atom at the vertex and the adsorbed molecule in the center of a pentagon is energetically rather unfavorable (due to lower packing density of the atoms than on the F layer), the activation energy is much higher.

On the P layer, the activation energies for the three rate-controlling steps for the hydrogenation of acetylene to vinyl, of vinyl to ethylene, and ethylene and ethyl on the (100) surface of the $Al_{13}Co_4$ compound are 63/61/80 kJ/mol, compared to a desorption energy of ethylene varying between 54 and 70 kJ/mol, depending on co-adsorbates. Except for the step from ethylene to ethyl, these energies are very similar to or even lower than the barriers calculated by Mei et al. [21] and by Studt et al. [11] for Pd(111) (66/74/72 kJ/mol – compared to a desorption energy of 82 kJ/mol). For Pd–Ag catalysts, the barriers are 66/10/61 kJ/mol. Although both the barrier for the formation of ethyl and the desorption energy are lowered by about 10 kJ/mol, hydrogenation remains slightly favored over desorption [21]. In this case, it was concluded that the factor governing selectivity is that the barrier for H-dissociation from ethyl back to ethylene is much lower than the barrier for ethyl hydrogenation to ethane. Here, we find that the decisive factor promoting the observed selectivity of the intermetallic compound is already the barrier for the hydrogenation of ethylene that is now much higher than the desorption barrier. This difference is driven by the change in the adsorption mode: On the surface of the intermetallic Co–Al compound, acetylene and vinyl are bound to two Al atoms in the pentagonal ring surrounding the Co atom (not on the Co atom itself !) and activated for hydrogenation (elongation of the C—C bond by 0.2 Å), while ethylene is weakly π-bonded on top of the Co atom and undergoes only a modest activation (elongation of the C—C bond by 0.07 Å). On the Pd–Ag catalysts, acetylene and ethylene are di-σ bonded irrespective of the surface composition [20]. However, for acetylene, both adsorption energy and C—C bond activation decrease strongly with increasing Ag content, whereas for ethylene, both adsorption energy and C—C bond length undergo only a modest change with alloy composition. Vinyl binds to the substrate in a di-σ configuration only if both C atoms can attach to a Pd surface atom, other-ways only the C–H group forms a surface bond. The dependence of the adsorption configuration on the Pd–Ag coordination explains the dramatic reduction in the activation energy for the hydrogenation of vinyl to ethylene. The binding of ethylene, however, shows no strong dependence on the Pd–Ag coordination and therefore alloying changes both activation energy for hydrogenation to ethyl and the desorption energy by about the same amount.

On the surface of the $Al_{13}Co_4$ catalyst, in contrast, the local structure of the active sites is always the same. The important point is that the active site, both for bonding and activating the hydrocarbon species and for the dissociative adsorption of hydrogen, is not the isolated transition-metal atom alone, but the entire, strongly covalently bonded pentagonal $CoAl_5$ complex: acetylene and vinyl bind to Al–Al bridge sites in this complex, atomic hydrogen to Al–Al bridges and Al–Co–Al hollows, only molecular hydrogen and ethylene adsorb on top of the Co atom. The increased adsorption capacity of the Al atoms is promoted both by strong, partially covalent Co–Al bonding in the PB's and by their reduced coordination at the edges of the stripes of Co–Al pentagons protruding from the surface.

The specific character of the surface atoms is also reflected in their local electronic structure. The electronic density of states (DOS) of bulk $Al_{13}Co_4$ is characterized by an Al band that has nearly free-electron character at large binding energies, but a very deep structure-induced DOS minimum at the Fermi level and a narrow Co-d band centered at about −2.4 eV below the Fermi level [32]. The local DOS of the Co and Al surface atoms is shown in Fig. 7. The peak of the Co-d band has been shifted to −1.8 eV, and a side-peak reflecting the strong binding to the surrounding Al atoms is found at −0.6 eV. In the Al DOS, we see a very strong resonance reflecting the hybridization between the Al-s,p and the Co-d states; the DOS minimum at the Fermi level has been filled by states of strongly hybridized character. Binding of the hydrocarbon species is promoted by the interaction of the C-p states with the Co–Al hybrid states.

Adsorption and dissociation occur on two different Co–Al pentagons (a direct dissociation of molecular hydrogen at a Co site already binding a hydrocarbon is energetically unfavorable) – it is therefore very important that the diffusion of atomic hydrogen requires only a very modest activation energy.

7. Conclusions

We have determined a detailed atomistic scenario for the selective hydrogenation of acetylene on the surface of the complex intermetallic compound $Al_{13}Co_4$ with isolated transition-metal

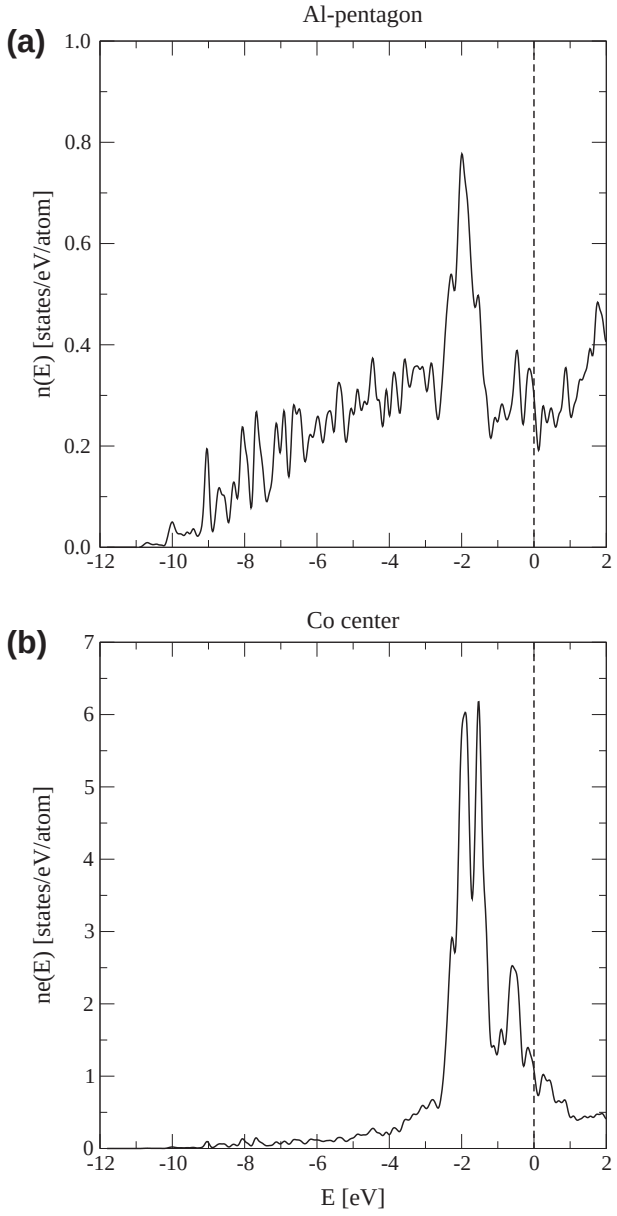

Fig. 7. Local electronic density of states of Al (a) and Co (b) atoms in the $CoAl_5$ pentagons exposed on the surface. Cf. text.

sites. Our studies confirm the usefulness of the concept of active-site isolation. However, our results also demonstrate that the active site is not the transition-metal alone, but the covalently bonded pentagonal $CoAl_5$ complex. The arrangement of the pentagonal clusters in zig-zag chains separated by wide troughs – and hence the topology of the surface – is very essential for promoting the high adsorption capacity of the Al atoms. The calculated adsorption energies and reaction barriers explain the high activity of the intermetallic compound as a hydrogenation catalyst, and the selectivity is determined by the qualitative difference in the adsorption configurations of acetylene and vinyl on one, and ethyl on the other side.

Our results refer to the as-cleaved surface of the intermetallic compounds and do not consider possible modifications of the surface, e.g. by oxidation. Such investigations have to be left to future work.

We expect that the scenario for the selective hydrogenation of acetylene on Pd–Ga or Ni–Zn catalysts will be very similar to that sketched here. In a PdGa compound with the B20 (FeSi-type) structure, each Pd atom is coordinated by seven Ga atoms only, suggesting that on the exposed surface, Pd atoms will be isolated. Remarkably, like $Al_{13}Co_4$ to decagonal Al–Co quasicrystals, the B20-phase of Pd–Al is also a lowest-order approximant to icosahedral Al–Pd–Mn quasicrystals [34]. However, for both alloys, no detailed structural characterization of the surface has been attempted as yet which could provide a basis for detailed simulations of the catalytic hydrogenation.

Acknowledgments

The work has been supported by the Austrian Ministry for Education, Science and Art through the Center for Computational Materials Science. M.K. thanks also for support from the Grant Agency for Science of Slovakia (No. 2/5096/25) and from the Slovak Research and Development Agency (Grant No. APVV-0413-06, CEX-Nanosmart).

References

[1] N.S. Schbib, M.A. Garcia, C.E. Gigola, A.F. Errazu, Ind. Eng. Chem. Res. 35 (1996) 1496.
[2] B.M. Collins, US Patent 4.126.645, 1978.
[3] T.V. Choudhary, C. Sivadinarayma, A.K. Datye, D. Kumar, D.W. Goodman, Catal. Lett. 86 (2003) 1.
[4] M.A. Volpe, P. Rodriguez, C.E. Cigola, Catal. Lett. 61 (1999) 27.
[5] K. Kovnir, M. Armbrüster, D. Teschner, T.V. Venkov, F.C. Jentoft, A. Knop-Gericke, Yu. Grin, R. Schlögl, Sci. Technol. Adv. Mater. 8 (2007) 420.
[6] J. Osswald, R. Giedigkeit, R.E. Jentoft, M. Armbrüster, F. Girgsdies, K. Kovnir, T. Ressler, Yu. Grin, R. Schlögl, J. Catal. 258 (2008) 210;
J. Osswald, K. Kovnir, M. Armbrüster, R. Giedigkeit, R.E. Jentoft, U. Wild, Yu. Grin, R. Schlögl, J. Catal. 258 (2008) 219.
[7] K. Kovnir, J. Osswald, M. Armbrüster, D. Teschner, G. Weinberg, U. Wild, A. Knop-Gericke, T. Ressler, Yu. Grin, R. Schlögl, J. Catal. 264 (2009) 93.
[8] K. Kovnir, M. Armbrüster, D. Teschner, T.V. Venkov, L. Szentmiklósi, F.C. Jentoft, A. Knop-Gericke, Yu. Grin, R. Schlögl, Surf. Sci. 603 (2009) 1784.
[9] D. Teschner, J. Borsodi, A. Wootsch, Z. Révay, M. Hävecker, A. Knop-Gericke, S.D. Jackson, R. Schögl, Science 320 (2008) 86.
[10] F. Studt, F. Abild-Pedersen, T. Bligaard, R.Z. Sørensen, C.H. Christensen, J.K. Nørskov, Angew. Chem. Int. Ed. 47 (2008) 9299.
[11] F. Studt, F. Abild-Pedersen, T. Bligaard, R.Z. Sørensen, C.H. Christensen, J.K. Nørskov, Science 320 (2008) 1320.
[12] M. Armbrüster, Yu. Grin, R. Schlögl, 1st Intern. Conf. on Complex Metallic Alloys and their Complexity, Nancy (France), vol. 4–7, 2009 (paper I11).
[13] M. Armbrüster, K. Kovnir, Yu. Grin, R. Schlögl, in: J.-M. Dubois, E. Belin-Ferr (Eds.), Complex Metallic Alloys: Fundamentals and Applications, Wiley-VCH, 2010, pp. 385–399.
[14] M. Armbrüster, K. Kovnir, Yu. Grin, R. Schlögl, P. Gille, M. Heggen, M. Feuerbacher, Ordered Cobalt–Aluminum and Iron–Aluminum Intermetallic Compounds as Hydrogenation Catalysts, EP09157875.7, 2009.
[15] M.K. Bhargava, A.A. Gadalla, K. Schubert, J. Less-Common Metals 42 (1975) 69.
[16] J. Grin, U. Burkhardt, M. Ellner, K. Peters, J. Alloys Compd. 206 (1994) 243.
[17] C. Freiburg, B. Grushko, R. Wittenberg, W. Reichert, Mater. Sci. Forum 228–231 (1996) 583.
[18] G. Nover, K. Schubert, J. Less-Common Metals 75 (1980) 51.
[19] F. Zaera, Phys. Rev. B 80 (2009) 914203;
F. Zaera, J. Phys. Chem. Lett. 1 (2010) 621.
[20] P.A. Seth, M. Neurock, C.M. Smith, J. Phys. Chem. B 107 (2003) 2009;
P.A. Seth, M. Neurock, C.M. Smith, J. Phys. Chem. B 109 (2005) 12499.
[21] D. Mei, P.A. Seth, M. Neurock, C.M. Smith, J. Catal. 242 (2006) 1;
D. Mei, M. Neurock, C.M. Smith, J. Catal. 268 (2009) 181.
[22] R. Addou, E. Gaudry, Th. Deniozou, M. Heggen, M. Feuerbacher, P. Gille, Yu. Grin, R. Widmer, O. Gröning, V. Fournée, J.-M. Dubois, J. Ledieu, Phys. Rev. B 80 (2009) 914203.
[23] G. Kresse, J. Furthmüller, Phys. Rev. B 54 (1996) 11169.
[24] G. Kresse, D. Joubert, Phys. Rev. B 59 (1999) 1758.
[25] J.P. Perdew, Y. Wang, Phys. Rev. B 45 (1992) 13244.
[26] G. Henkelman, H. Jónsson, J. Chem. Phys. 111 (1999) 7010.
[27] C.L. Henley, J. Non-Cryst. Solids 153-154 (1993) 172.
[28] P. Jeglič, M. Heggen, M. Feuerbacher, B. Bauer, F. Haarmann, J. Alloys Compd. 480 (2009) 141.
[29] P. Jeglič, S. Vrtnik, M. Bobnar, M. Klanjšek, B. Bauer, P. Gille, Yu. Grin, F. Haarmann, J. Dolinšek, Phys. Rev. B 82 (2010) 104201.
[30] B. Grushko, C. Freiburg, K. Bickmann, R. Wittenberg, Z. Metallkd. 88 (1997) 379.
[31] M. Mihalkovič, M. Widom, Phys. Rev. B 75 (2007) 014207.
[32] M. Krajčí, J. Hafner, Phys. Rev. B 62 (2000) 243.
[33] J. Dolinšek, M. Komelj, P. Jeglič, S. Vrtnik, D. Stanic, P. Popčevic, J. Ivkov, A. Smontara, Z. Jagličic, P. Gille, Yu. Grin, Phys. Rev. B 79 (2009) 184201.
[34] M. Krajčí, J. Hafner, Phys. Rev. B 75 (2007) 024116.